ELSEVIER

Journal of Chromatography A, 670 (1994) 1–14

JOURNAL OF CHROMATOGRAPHY A

Comparative evaluation of adsorption energy distribution functions obtained by analytical and numerical methods

Sadroddin Golshan-Shirazi[☆], Georges Guiochon*

Department of Chemistry, University of Tennessee, Knoxville, TN 37996-1503, USA and Division of Analytical Chemistry, Oak Ridge National Laboratory, Oak Ridge, TN 37831-6120, USA

(First received April 21st, 1993; revised manuscript received December 31st, 1993)

Abstract

The adsorption energy distributions derived from the Adamson and Ling (AL), and the House and Jaycock HILDA numerical methods are compared with the Sips analytical solution, which is used as a benchmark for these numerical methods. Excellent agreement between the analytical and numerical methods is achieved provided that the isotherm data are measured over a wide range of adsorbate partial pressures, extending to near the saturation capacity. While a lack of accurate low-pressure data will merely result in an inaccurate energy distribution in the high-energy range, a lack of these high-pressure data may result in an entirely wrong energy distribution.

1. Introduction

Almost all solid surfaces are heterogeneous [1,2]. A quantitative description of adsorption on a real, heterogeneous adsorbent requires the use of the adsorption energy distribution function [1]. Two widely different models of the adsorbent surface have been discussed in the literature [3,4]. The random distribution site model introduced by Hill [3] assumes that sites with different adsorption energy are randomly distributed over the surface, and the adsorption system must be considered as a single thermodynamic entity. The homotattic model [4] assumes that the surface is made of patches randomly distributed on the surface, but that each patch is covered with adsorption sites having the same adsorption energy, *i.e.*, is homogeneous. These patches are large enough to permit the application of statistical thermodynamics to every one of them, so the whole system can be considered as a collection of independent subsystems.

In this work, we consider the latter, patch-wise heterogeneity model in which the average degree of surface coverage at constant temperature, $q^d(p)$, is related to the partial pressure, p, of the adsorbate vapor by

$$q^d(p) = \frac{q(p)}{q_s} = \int_{\epsilon_{min}}^{\epsilon_{max}} \theta(\epsilon, p) f(\epsilon)\, d\epsilon \qquad (1)$$

where $q(p)$ is the experimental adsorption isotherm, q_s the monolayer saturation capacity of the adsorbent, $\theta(\epsilon, p)$ the local isotherm on the homogeneous patch having an adsorption energy

* Corresponding author. Address for correspondence: Department of Chemistry, University of Tennessee, Knoxville, TN 37996-1503, USA.

☆ Present address: AAI, Wilmington, NC, USA.

0021-9673/94/$07.00
SSDI 0021-9673(94)00073-I

ϵ and $f(\epsilon)$ the energy distribution function, so $f(\epsilon)\,d\epsilon$ is the fraction of the surface on which the binding energy is between ϵ and $\epsilon + d\epsilon$. ϵ_{min} and ϵ_{max} are the lowest and the highest values of the adsorption energy on the heterogeneous surface considered, respectively.

The aim of this approach is the derivation of the energy distribution function, $f(\epsilon)$, from the experimental isotherm, $q(p)$ (which is the only parameter in Eq. 1 which can be determined experimentally), and assuming a model for the local isotherm, $\theta(\epsilon, p)$. It has been extensively used in the past 20 years to investigate real surfaces [1,2,5]. A number of different solutions of Eq. 1 have been suggested. However, few comparisons, if any, have been made between the results obtained when applying these different solutions to the same set of data.

There are two general types of solutions for such a problem, analytical and numerical. Analytical solutions can be derived only if further assumptions are made regarding both the local and the experimental isotherm models. These assumptions are too restrictive to be of practical value, so attention has mainly focused on numerical solutions. This approach requires less restrictive assumptions, regarding only the local isotherm model. However, it suffers from a considerable drawback. Numerical methods are essentially empirical, using computing power to derive the energy distribution function which permits the calculation of the isotherm that best approximates the experimental isotherm. The mathematical problem is ill-posed, however, and does not have a unique solution [1,2,5–9], so restrictions are necessary. Because there are no independent methods for the determination of the adsorption energy distribution function, and there are no adsorbents available with a known adsorption energy distribution function, we have no way of knowing whether the result of the calculation is correct. Therefore, the reliability of any procedure for the experimental determination of the adsorption energy distribution function is in doubt.

In this paper, we consider the analytical solutions of Eq. 1 and compare them with the numerical solutions available for the evaluation of the adsorption energy distribution function from experimental isotherms. This work will provide further information on the sensitivity of the distribution function to the choice of a model for the experimental isotherm, to the accuracy of the experimental data and to the numerical errors.

2. Theory

From a mathematical point of view, Eq. 1 is a Fredholm integral equation of the first kind, for which there is no general analytical solution. The problem is ill-posed and does not have a unique solution, so further restrictions are necessary to obtain the solution of the physical problem. Two types of methods have been investigated in attempts to derive a solution, numerical methods based on iterative procedures and direct analytical methods, which require some further assumptions and simplifications. In all instances, an isotherm model must be assumed for the local adsorption isotherm. We discuss first analytical and then numerical solutions.

2.1. Analytical solution of the Sips method

Three different methods for the determination of an analytical solution of Eq. 1 have been suggested, the Sips [10], Hobson [11] and condensation approximation [12] methods. These methods differ mainly in the local isotherm model assumed. In the Sips method, the local isotherm is the Langmuir model: the adsorption is localized, the adsorbate does not move on the surface, there are no adsorbate–adsorbate interactions and the gas phase is ideal. As this method uses the least simplistic local model, it is the only method considered here.

The local isotherm is given by

$$\theta(\epsilon, P) = \frac{P}{P + K\,e^{-\epsilon/RT}} \tag{2}$$

where K is a constant independent of ϵ, of the column temperature T and of the location on the surface. The following equations have been

suggested in the literature to provide an estimate of the value of K:

$$K = \frac{\sqrt{MT}\sigma_m}{3.5 \cdot 10^{22} t_0} \quad (3a)$$

$$K = 1.76 \cdot 10^4 \sqrt{MT} \quad (3b)$$

$$K = P_s e^{\Lambda_v / RT} \quad (3c)$$

where M is the molecular mass of the adsorbate, σ_m the monolayer coverage (number of molecules per unit surface area of adsorbent), t_0 the vibration time of the adsorbed molecules (s); P_s the vapor pressure, Λ_v the molar heat of vaporization of the adsorbate studied and R the ideal gas constant (1.987 cal/K · mol) (1 cal = 4.186 J). With the numbers used, K in Eqs. 3a and 3b is given in Torr (1 Torr = 133.322 Pa).

The first equation is based on the kinetic derivation of the Langmuir isotherm, which equates at equilibrium the adsorption and desorption flux, assuming the condensation coefficient to be unity [11,13]. The second was suggested by Hobson [11] for nitrogen and the third by Dormant and Adamson [14]. In this work, we used Eq. 3c.

Eq. 1 is reformulated as a Stieltjes transform of the distribution function, which is inverted using standard mathematical techniques [15]. Inserting Eq. 2 into Eq. 1, and letting

$$y = \frac{K}{P} + 1 \quad (4a)$$

$$x = \exp(\epsilon / RT) \quad (4b)$$

$$g(x) = f[RT \ln(1 + x)] = f(\epsilon) \quad (4c)$$

$$h(y) = \frac{1}{RT} q^d\left(\frac{K}{y - 1}\right) \quad (4d)$$

we obtain for Eq. 1

$$h(y) = \int_0^\infty \frac{g(x)}{x + y} \quad (4)$$

Thus, $h(y)$ is the Stieltjes transform of $g(x)$, and the solution is [15]

$$f(\epsilon) = g(x) = \frac{h(x e^{-i\pi}) - h(x e^{i\pi})}{2i\pi} \quad (5)$$

For obvious physical reasons, the limits of $q^d(P)$ have following values:

$$q^d(0) = 0 \quad \text{and} \quad \lim_{P \to \infty} q^d = 1 \quad (6)$$

The first condition is always satisfied; the second one is also, provided that the function $f(\epsilon)$ is normalized, *i.e.*, if

$$\int_0^\infty f(\epsilon)\, d\epsilon = 1 \quad (7)$$

To go further and determine $f(\epsilon)$, we need an analytical expression for the experimental isotherm. This equation must satisfy Eq. 6. Thus, for example, we can use the Langmuir model but not the Freundlich model, which does not satisfy the second limit condition. Usually, the Langmuir model does not fit well the experimental data measured with heterogeneous surfaces [1,2]. It is possible to derive an adsorption energy distribution function with the Sips method for only few local isotherm models.

Generalized Freundlich isotherm

This isotherm is given by

$$q^d(P) = \left(\frac{P}{P + K}\right)^c \quad (8)$$

where c is a numerical parameter and K is the same as in Eq. 2. Unlike the Freundlich isotherm, the generalized Freundlich isotherm satisfies the second condition in Eq. 6, if $0 < c < 1$. In this case, the adsorption energy distribution function is given by

$$f(\epsilon) = \frac{1}{RT} \cdot \frac{\sin \pi c}{\pi} (e^{\epsilon / RT} - 1)^{-c} \quad (9)$$

This result is easily extended to the generalized form of the isotherm in Eq. 8:

$$q^d(P) = \left(\frac{P}{P + A}\right)^c \quad (10)$$

with $A < K$. The adsorption energy distribution function for the isotherm in Eq. 10 is given by [10]

$$f(\epsilon) = 0 \quad 0 < \epsilon < \epsilon_0 \quad (11a)$$

$$f(\epsilon) = \frac{1}{RT} \cdot \frac{\sin \pi c}{\pi} [e^{(\epsilon - \epsilon_0)/RT} - 1]^{-c} \quad \epsilon_0 < \epsilon \tag{11b}$$

where $\epsilon_0 = RT \ln(K/A)$. Thus, the replacement of K by A merely shifts the adsorption energy distribution by the amount ϵ_0.

Langmuir isotherm

In this case, $c = 1$ in Eqs. 10 and 11, and the latter reduces to a δ function, the distribution being zero everywhere, except for $\epsilon = \epsilon_0$, where it is infinite. This result is consistent with the Langmuir isotherm model which assumes a homogeneous surface, all the adsorption sites having the same adsorption energy, ϵ_0.

Multi-Langmuir isotherm

Many experimental data can be fitted to a bi-Langmuir or a multi-Langmuir isotherm equation [16,17]:

$$q^d(P) = \frac{1}{q_s} \sum_i q_{s,i} \frac{P}{P + A_i} \tag{12}$$

Applying the same calculation procedure as above, we obtain that the adsorption energy distribution is zero everywhere, except at the energies

$$\epsilon_i = RT \ln \frac{K}{A_i} \tag{13}$$

where it is infinite. In practice, the adsorption energy distribution for a multi-Langmuir isotherm consists of a series of very sharp lines. The surface is made of homogeneous patches of a few different types. The number of lines is equal to the number of patch types, their energy to the adsorption energy on the corresponding adsorption site and the relative intensity of the impulse is $q_{s,i}/q_{s,tot}$, where $q_{s,i}$ is the saturation capacity of the corresponding Langmuir term and $q_{s,tot}$ is the total saturation capacity. This result is consistent with the multi-Langmuir isotherm model.

Misra isotherm

This isotherm is given by [18]

$$q^d(P) = \frac{np}{(K - np)\ln(1 + n)} \cdot \ln\left(\frac{1 + \frac{K}{P}}{1 + n}\right) \tag{14}$$

and the corresponding adsorption energy distribution is [18]

$$f(\epsilon) = \frac{n}{RT \ln(1 + n)} (n + e^{\epsilon/RT})^{-1} \tag{15}$$

If ϵ_0 is the lower limit of the adsorption energy distribution, the isotherm and the adsorption energy distributions become, respectively [18],

$$q^d(P) = \frac{np}{(K - np)\ln\left(1 + \frac{n}{r}\right)} \cdot \ln\left(\frac{r + \frac{K}{P}}{r + n}\right) \tag{16}$$

$$f(\epsilon) = \frac{n}{RT \ln(r + n) - \epsilon_0} (n + e^{\epsilon/RT})^{-1} \tag{17}$$

with $r = e^{\epsilon_0/RT}$. According to Eq. 11, $f(\epsilon)$ tends towards zero when ϵ increases indefinitely, it increases with decreasing ϵ and increases indefinitely when ϵ tends towards ϵ_0. The adsorption energy distribution is zero at values of ϵ below ϵ_0.

Dubinin–Radushkevich isotherm

The empirical Dubinin–Radushkevich isotherm [19] is given by

$$q^d(P) = \exp\left[-B'\left(RT \ln \frac{P_s}{P}\right)^2\right] \tag{18}$$

where B' is a numerical constant and P_s is the vapor pressure of the pure liquid adsorbate at the temperature of the experiment. Like the Freundlich isotherm, the Dubinin–Radushkevich isotherm does not satisfy Eq. 6, as required for the Stieltjes transform, and is not physically compatible with the Sips method. Misra modified the Dubinin–Radushkevich isotherm and proposed a "generalized" equation that satisfies the requirements of the Stieltjes transform. This new isotherm equation is [20]

$$q^d(P) = \exp\left\{-B\left[RT \ln\left(1 + \frac{c}{P}\right)\right]^2\right\} \tag{19}$$

where B and c are numerical constants. With the addition of 1 in the expression under the logarithm operator, Eq. 6 is satisfied, and the replacement of P_s by an adjustable constant gives some flexibility to an empirical equation; c is obtained by fitting the experimental data to

Eq. 19. The adsorption energy distribution function is

$$f(\epsilon) = \frac{\exp(\pi^2 BR^2T^2)}{\pi RT} \cdot \sin(2\pi RTB\epsilon)\, e^{-B\epsilon^2} \quad (20a)$$

The shape of the adsorption energy distribution obtained is very different from that given in Eq. 11. $f(\epsilon)$ tends towards 0 when ϵ tends towards either 0 or ∞. The profile is a skewed Gaussian reaching its maximum value for

$$\epsilon = \epsilon_M = \frac{1}{\sqrt{2B}} \quad (20b)$$

2.2. Numerical solutions

With all numerical methods, a local isotherm model needs to be assumed for each patch. This means that a general model of the local isotherm (*e.g.*, Langmuir) must be assumed, in addition to a functional relationship between the coefficients of this isotherm and the adsorption energy. Because of the ill-posed nature of the mathematical problem and the non-unicity of its general solution [6–9], two approaches have been used to calculate numerical solutions of Eq. 1. In the first approach, a particular form of the adsorption energy distribution function is assumed. Its coefficients are determined by matching the isotherm calculated with Eq. 1 to the experimental isotherm, and minimizing the residue with a conventional fitting procedure. In the second approach, no assumptions are made regarding the nature or shape of the adsorption energy distribution function, and this function is derived directly from the experimental isotherm. This type of computation is extremely difficult, however, because of the constraints imposed by the requirement of a realistic solution and the influence of experimental errors.

Methods based on the assumption of an analytical function for the adsorption energy distribution

Several groups have investigated this approach in the past. Ross and Oliver [4] assumed a Gaussian distribution function for the adsorption energy distribution. Their method can also be used with the sum of a few Gaussian distributions. Hoory and Prausnitz [21] used a long-tail function, skewed and defined only for positive values of ϵ. Kindel [22] assumed a Maxwell function, Jaroniec *et al.* [23] a gamma function and Sparnaay [24] a surface covered by a few patches only.

In general, any kind of analytical expression can be assumed for the energy distribution, and the coefficients of this expression can be obtained by optimization, using any of a variety of curve-fitting algorithms. For example, Van Dongen [25] assumed an analytical expression for the energy distribution of the form

$$\ln f(\epsilon) = b_0 + b_1\epsilon + b_2\epsilon^2 + \cdots + b_n\epsilon^n \quad (21)$$

The optimum values of the parameters b_i are obtained by minimizing the sum of the squares of the differences between calculated and experimental isotherm points with respect to the b_i.

The major disadvantage of this approach is that there are no methods available for the direct determination of the adsorption energy distribution, or any fundamental or even compelling reasons to chose any one of the many possible distribution functions available. The use of this approach was a practical necessity when the computing power available was low, and it has become obsolete with the advent of modern computers that permit the much more complex calculations required when no energy distributions are assumed.

Direct methods of calculation of the adsorption energy distribution

Three different, important procedures have been described in the literature, the Adamson and Ling (AL) method [26], the HILDA algorithm of House and Jaycock [27] and the CAEDMON algorithm of Ross and Morrison [28]. None of them makes any *a priori* assumption regarding the shape of the adsorption energy distribution, except that $f(0) = 0$, $f(\epsilon)$ tends towards zero when ϵ tends towards infinity and that the integral over the whole energy range is finite. We discuss these methods successively.

Adamson–Ling method. In this method [26], Eq. 1 is rewritten as

$$q^{d}(p) = \int_{0}^{1} \theta(\epsilon, p)\, dF \tag{22a}$$

with

$$F(\epsilon) = \int_{\epsilon_{min}}^{\epsilon_{max}} f(\epsilon)\, d\epsilon \tag{22b}$$

where $F(\epsilon)$ is the integral site energy distribution, *i.e.*, the fraction of the surface covered by sites on which the adsorption energy exceeds ϵ. Eq. 22a can be approximated by the sum

$$q_{dj} = \sum_{i=1}^{i=n} \theta_{ji}(F_i - F_{i-1}) \quad j = 1, 2, \ldots, m \tag{23}$$

where m is the number of data points acquired and n is the number of intervals used to represent the adsorption energy distribution. An iterative calculation procedure is used. The first approximation of the integral of the adsorption energy distribution for this iterative procedure is obtained by using the condensation approximation for the local isotherm:

$$q_{dj} = \int_{0}^{F(\epsilon_j)} 1 \times dF(\epsilon) + \int_{F(\epsilon_j)}^{1} 0 \times dF(\epsilon) \tag{24}$$

Hence, the first approximation of the energy integral is given by

$$F(\epsilon_j) = q_{dj_{exp}} \tag{25}$$

These values of the integral of the adsorption energy distribution are used in Eq. 22, together with a realistic model of the local isotherm, to evaluate the total isotherm, $q_{dj_{cal}}$. The monolayer capacity should be evaluated independently, for example from the results of the BET method.

In their original work, performed in 1961, Adamson and Ling [26] had to use a graphical procedure to judge the deviations between the calculated and the experimental isotherms, make the decisions regarding the extent of the disagreement and the nature of the adjustments best needed for the next iteration step. Difficulties arose because the distribution resulting from successive approximations may not differ much from one step to the next, the changes may not be systematic and no continuous trend towards convergence was apparent. The graphical method showed also a tendency for ripples to appear in the energy distribution function, and to propagate. These ripples have to be damped and suppressed, so the final distribution function is not oscillating. Later, a computer program was developed to carry out the method, and the computation was ended when the root mean square of the deviation between the experimental and the calculated isotherms became smaller than a certain threshold.

HILDA algorithm. House and Jaycock [27] proposed a numerical method based on the iterative scheme of Adamson and Ling [26]. This method was presented under the acronym HILDA, for Heterogeneity Investigated at Loughborough by a Distribution Analysis. Instead of directly evaluating the Eq. 22, House and Jaycock rewrote it as

$$q^{d}(p_j) = \int_{0}^{1} F(\epsilon)\, d\theta(\epsilon, p_j) \tag{26}$$

They assumed that the energy distribution has a finite width, determined by the lowest and highest partial pressures at which adsorbed amounts have been determined experimentally, that any surface patch which has an integral adsorption energy greater than ϵ_{max} is fully covered with a monolayer of adsorbate, while any surface patch for which the integral adsorption energy is lower than ϵ_{min} is empty. Then, Eq. 26 can be rewritten as

$$q^{d}(p_j) = \int_{\theta_l(p_j)}^{\theta_h(p_j)} F(\epsilon)\, d\theta(\epsilon, p_j) + F(\epsilon_{min})\theta_l p_j + F(\epsilon_{max})[1 - \theta_h(p_j)] \tag{27}$$

where θ_h and θ_l are the fractional coverages at the pressure p_j of the surface patches with the highest and lowest adsorption energies, respectively. As in the AL method, the condensation approximation is used for obtaining the initial value of the integral energy, F, and the value of F in the kth iteration is calculated according to

$$F^k(\epsilon_j) = \frac{q^d_{j_{exp}}}{q^d_{j_{cal}}} \cdot F^{k-1}(\epsilon_j) \quad (28)$$

The solution is reached when the root mean square deviation between the experimental and the calculated isotherms becomes lower than a given threshold.

The algorithm includes also a quadratic smoothing function for the isotherm data. This function can also be used to smooth the energy distribution function obtained, if necessary. In order to ensure that an evenly spaced adsorption energy distribution function will be obtained, the program does not use the experimental adsorption isotherm, under its classical representation, but with the adsorbate partial pressure expressed in a logarithmic scale. The HILDA program offers four choices for the local isotherm, the Langmuir, the Fowler–Guggenheim, the Hill–de Boer or the virial isotherms. Independent, prior knowledge of the monolayer capacity of the adsorbent is not a prerequisite for the calculation. The value of the monolayer capacity can be adjusted and eventually determined from the normalization factor, since $F(\epsilon_{min}) = \int_{\epsilon_{min}}^{\epsilon_{max}} f(\epsilon)\, d\epsilon$ has to be equal to 1. The HILDA algorithm has been used extensively for the investigation of the surface heterogeneity of various solids [29].

CAEDMON algorithm. Ross and Morrison [28] developed another algorithm for the same purpose, the Computer Adsorptive Energy Distribution in the MONolayer (CAEDMON). This algorithm uses only the two-dimensional virial isotherm to represent the local isotherm. This algorithm was later modified by Sacher and Morrison [30], who used more reliable and effective procedures to ensure convergence and uniqueness of the solution.

Quasi-Adamson method. Roles and Guiochon [17] used a combination of two approaches developed previously. In a first part, they used a modification of the AL method, with computerized numerical iterations. The experimental isotherm is replaced by a multi-Langmuir isotherm. In most cases, a bi-Langmuir isotherm was found to fit the experimental data excellently. As we have shown in the previous section, this algorithm is not necessary since for a multi-Langmuir experimental isotherm there is an analytical solution of Eq. 1, a series of impulses, one for each Langmuir term of the isotherm, at energies related to the coefficients of the Langmuir term. Although in a second, confirmation stage the method [17,31,32] replaces the multi-Langmuir isotherm by an Akima spline [33] representation of the experimental data to verify the number of modes of the energy distribution, it cannot divorce itself from the multi-Langmuir representation used in the first stage. Because isotherm measurements can be made only in a limited range of partial pressures, a multi-Langmuir isotherm still has to be used for the extrapolation of the experimental data at high pressures. As a consequence, the method may generate spurious peaks.

The second part of this procedure, called the Distribution Function Substitution, is similar to the method developed by Ross and Oliver [4]. Each peak of the energy distribution function derived in the first part of the procedure is replaced by an analytical function. If the peak obtained from the quasi-Adamson method is symmetrical, it is replaced by a Gaussian distribution; if slightly skewed, by an exponentially modified Gaussian distribution; and if highly unsymmetrical, by a Γ function. The parameters of these functions are adjusted and optimized by a simplex optimization pursued until the best fit is obtained between the experimental and calculated isotherms, using a test based on the value of the root mean square of the difference between measured and calculated isotherms.

In practice, this method suffers the same drawbacks as the Ross and Oliver approach [4]. It involves the replacement of the unknown adsorption energy distribution by the sum of a number of analytical functions, and the optimization of their parameters. Admittedly, the selected distributions are somewhat less arbitrarily chosen than those elected by Ross and Oliver [4], and by those following the same approach [21–25], but that still does not make the method realistic, since there are no reasons at this stage

to select any model for the adsorption energy distribution.

Algorithms selected for the calculation of the adsorption energy distribution

For further numerical calculations, we decided to select the Adamson and Ling [26] and the House and Jaycock [27] approaches, which make no arbitrary choices of either an isotherm model for the experimental isotherm or a distribution model for the adsorption energy distribution. We used slightly modified algorithms implementing the essential principles of the AL [26] and HILDA [27] original methods, and wrote computer programs to implement them. As the computers available to us are considerably more powerful than those available to these authors, numerical procedures can be more sophisticated and calculations pursued for orders of magnitude larger numbers of iterations. This contributes to considerable improvements in the quality of the results available and permits detailed comparisons between results of the two methods. Further, as there are isotherms for which an analytical solution does exist, we can design a quality benchmark for numerical solutions by calculating them in cases when the analytical solution exists and comparing both solutions.

In both algorithms, we assumed the local isotherm to be given by the Langmuir model (Eq. 2). This assumption is not a restriction; both programs could be used with any local isotherm model making physical sense. The Langmuir model is appropriate for a comparison between the results of various calculation methods.

Algorithm based on the AL method. This first algorithm is similar to the one designed by Roles and Guiochon [17], with the following differences:

(i) The experimental isotherm is used directly, and not replaced by a model.

(ii) We introduce q_s in Eq. 1, which provides the distribution $f(\epsilon)$, while they ignored it [17], with the result that this earlier algorithm gives $q_s f(\epsilon)$.

(iii) Instead of using Eq. 1 directly in the calculation [17], we replaced it by Eq. 22, as did Adamson and Ling [26]. The advantage is that the method requires only the use of the integral distribution, $F(\epsilon)$, in the calculation. As $F^k(\epsilon)$ is calculated from $F^{k-1}(\epsilon)$, there is no need to calculate $f(\epsilon)$, except once, at the very end of the program. In contrast, procedures using Eq. 1 require $f(\epsilon)$ to calculate q^d_{cal} at each iteration. This in turn requires the fitting of $F^{k-1}(\epsilon)$ with an Akima cubic spline [33], and differentiation of the spline. This change results into faster calculations and the possibility to carry out longer iterations.

(iv) As $F(\epsilon)$ must obviously be found within the interval 0–1, we introduce this condition in the program, by replacing systematically any negative value by 0, and any value larger than 1 by 1 at each iteration. This latter restriction has a profound positive influence on the shape of the adsorption energy distribution when the number of iterations is small or moderate and it hastens convergence (see Fig. 1).

(v) We found that a very large number of iterations has to be carried out. Some calculations reported below include up to 20 000 such iterations, whereas earlier results included no more than 200 [17]. The width of the energy distribution decreases slowly with increasing numbers of iterations (see below), especially when the energy distribution has sharp peaks. Hence the number of iterations needed for accurate results becomes very large when almost homogeneous surfaces are studied.

Algorithm based on the HILDA method. The algorithm developed includes only two modifications to the original HILDA algorithm:

(i) Since, as mentioned in the previous section, $F(\epsilon)$ must be found within the interval 0–1, we included this restriction in this program also. At the end of each iteration, any negative value is replaced by 0, any value larger than 1 by 1.

(ii) Since in any iteration, k, $F^k(\epsilon)_{j+1}$ must be larger than $F^k(\epsilon)_j$, for any data point j, the following statement is included in the program:

$$\begin{aligned} &\text{if} \quad F^c(\epsilon)_{j+1} < F^c(\epsilon)_j \\ &\text{then} \quad F^c(\epsilon)_{j+1} = F^c(\epsilon)_j \end{aligned} \tag{29}$$

instead of $F^c(\epsilon)_{j+1} = F^c(\epsilon)_j + 1 \cdot 10^{-6}$ as used by House and Jaycock [26]. The number $1 \cdot 10^{-6}$ is arbitrary. We found that when the number of iterations is small, the shape of the distribution changes somewhat with the value chosen for that small number, and we preferred to replace it by zero.

3. Results and discussion

We compared the adsorption energy distributions obtained with the two numerical solutions and the Sips analytical solution in the cases when the experimental isotherm is a Langmuir and a Misra isotherm.

3.1. The experimental isotherm is a Langmuir isotherm

In this case the analytical solution is a single impulse, or Dirac δ function at the energy $\epsilon = RT \ln(K/A)$. The comparison between this solution and the numerical solutions will be instructive regarding the ability of the program to handle discontinuities. Numerical solutions always include some dispersion of numerical origin, related to the computer need to round-up numbers, and programs experience great difficulties in accounting for discontinuities or impulses. To perform the comparison, we selected a value $A = 0.0013$ atm, and $K = 36\,450$ atm, which gives as solution an impulse at $\epsilon = 10.66$ kcal/mol.

Fig. 1 shows the results obtained with different algorithms, all run for the same number of iterations (2000). The vertical solid line gives the analytical solution. The dotted line is the numerical solution given by the HILDA method, while the dashed line results from the AL method. Note that both algorithms include the condition that $F(\epsilon)$ cannot exceed 1. The AL and HILDA solutions are almost exactly overlaid, and cannot be distinguished, except at the very top. Note that the energy range used for the figure is only 1 kcal/mol. Two other solutions are shown in Fig. 1, the solution given by the HILDA algorithm without the added restrictions regarding the value of $F(\epsilon)$ which cannot exceed

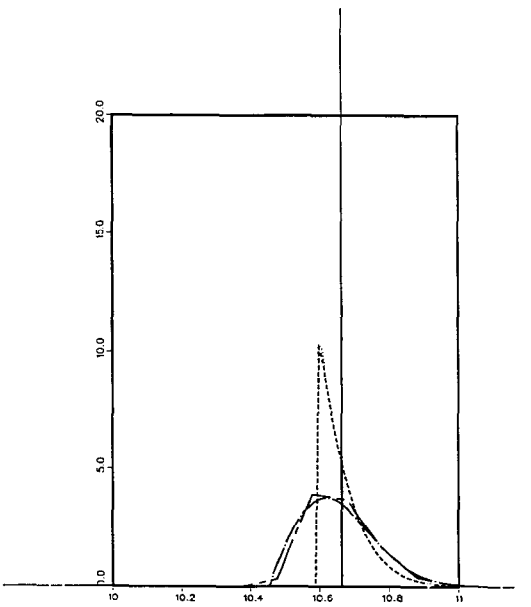

Fig. 1. Comparison of the analytical and several numerical solutions obtained for the adsorption energy distribution in the case when the experimental isotherm follows the Langmuir model. Abscissa, adsorption energy (kcal/mol). Ordinate, energy ditribution (mol/kcal). Solid line, analytical solution, a δ-function at $\epsilon = RT \ln(K/A)$ (Eq. 13); dotted line, numerical solution calculated with our implementation of the HILDA algorithm [26]; dashed line, numerical solution calculated with our implementation of the Adamson and Ling [25] algorithm; dot–chain line (–·–), numerical solution calculated with the original HILDA algorithm [26], without the restriction added by us [if $F(\epsilon) > 1$, then $F(\epsilon) = 1.0$]; dashed–chain line (–––), numerical solution calculated with the "quasi-Adamson" algorithm of Roles and Guiochon [16]. In all the numerical calculations, the number of iterations is equal to 2000.

1 (–·– line), and the Roles–Guiochon algorithm (––– line). These last two lines are very close.

These results demonstrate the profound similarity between the AL [26] and HILDA [27] methods. They also show the significant improvement brought by our simple correction to these methods [If $F(\epsilon) < 0$, $F(\epsilon) = 0$; if $F(\epsilon) > 1$, $F(\epsilon) = 1$], resulting in a numerical solution which is much sharper on the low-energy side, and closer to the analytical solution, although still significantly different on the high-energy side. The results obtained with the quasi-Adamson method [17,31] are slightly different from those given by the AL method or the HILDA algo-

rithm, probably because in this calculation procedure $f(\epsilon)$ is calculated at each iteration step, by fitting the values of $F(\epsilon)$ to an Akima cubic spline and differentiating the spline. This procedure causes errors of numerical origin which remain significant as long as the number of iterations is not very large.

A further improvement could be made by increasing the number of iterations. We compare in Fig. 2 the analytical solution (solid line) and the numerical solution derived from the HILDA algorithm (dotted line) after 20 000 iterations. The numerical solution has become much narrower, and is now very close to the analytical solution.

Finally, in Fig. 3, we compare the analytical solution obtained for a bi-Langmuir isotherm (solid lines) and the numerical solution calculated with the HILDA algorithm, and 20 000 iterations (dotted line). For a multi-Langmuir isotherm, the solution is a series of impulses. The number of impulses is the number of terms in the isotherm model; their location is given by Eq. 13. The numerical solution has two narrow peaks. The numerical dispersion is more im-

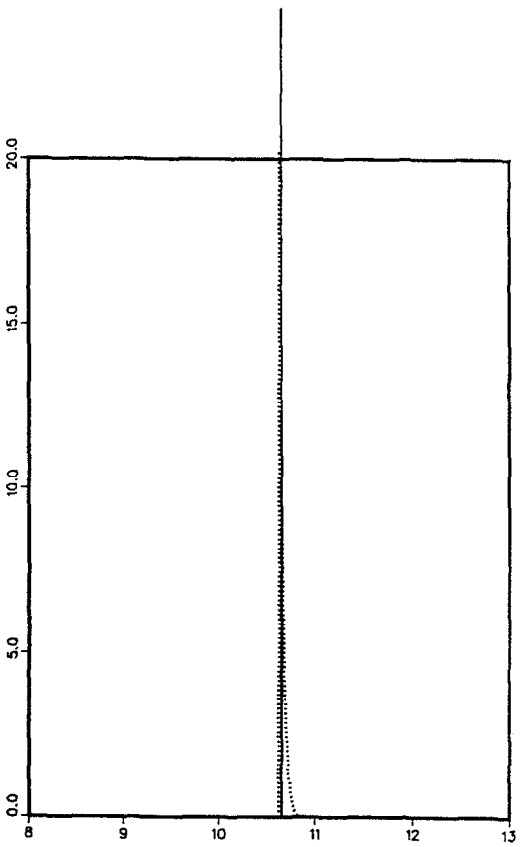

Fig. 2. Comparison of the analytical and numerical solutions obtained for the adsorption energy distribution in the case when the experimental isotherm follows the Langmuir model. Abscissa, adsorption energy (kcal/mol). Ordinate, energy distribution (mol/kcal). Solid line, adsorption energy distribution calculated from the analytical solution (Eq. 13); dotted line, adsorption energy distribution calculated with our implementation of the HILDA algorithm [26]. The number of iterations for this numerical solution is 20 000.

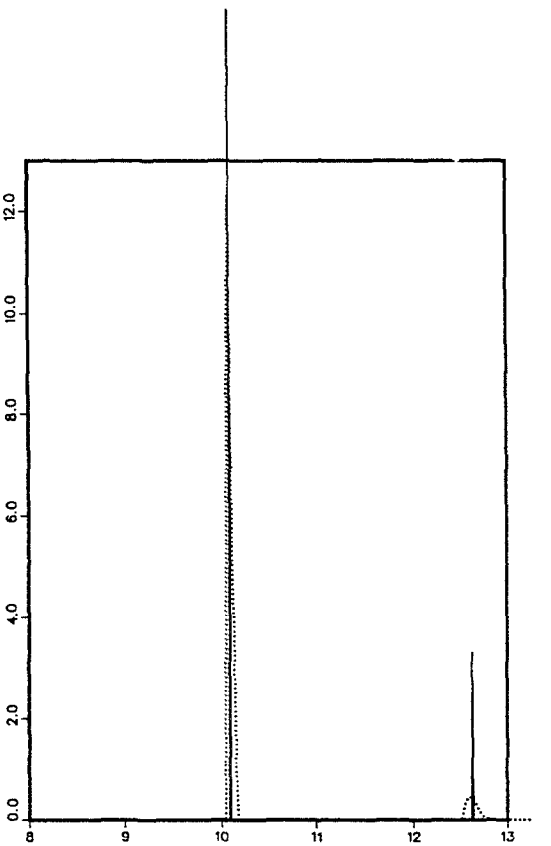

Fig. 3. Comparison of the analytical and numerical solutions obtained for the adsorption energy distribution in the case when the experimental isotherm follows a bi-Langmuir model. Abscissa, adsorption energy (kcal/mol). Ordinate, energy distribution (mol/kcal). Solid line, adsorption energy distribution obtained from the analytical solution (Eq. 13); dotted line, energy distribution calculated with our implementation of the HILDA algorithm [26]. The number of iterations is 20 000.

portant for the higher energy than for the lower energy impulse.

3.2. The experimental isotherm is a Misra isotherm

With the Misra isotherm [18] also, the adsorption energy distribution can be derived as an analytical solution to Eq. 1. This solution is a broad distribution which provides a different test of the validity of the numerical algorithms. The Misra isotherm is given by Eq. 16 and the corresponding adsorption energy distribution by Eq. 17. In the calculations, we assumed that $n = 5$, $\epsilon_0 = 1$ kcal/mol, and $K = 36\,450$ atm. Using the isotherm given by Eq. 16 as an experimental isotherm, we also calculated the adsorption energy distributions using the AL and the HILDA algorithm.

The adsorption energy distributions calculated with the AL and the HILDA algorithms are compared in Fig. 4. They are nearly identical. In Fig. 5, we compare these two distributions, represented by the solution of the HILDA algorithm (dotted line), and the analytical solution given by Eq. 17 (solid line). The two results are in very good agreement, in spite of a slight smoothing of the energy discontinuity at ϵ_0 which is replaced by a steep decay, and a rounding up of the energy maximum. This completes the demonstration that if the AL and HILDA algorithms are carried out with a sufficiently large number of iterations, they give an accurate solution of Eq. 1, and can provide the correct energy distribution, provided that the isotherm data made available to the programs contain all the required information, *i.e.*, cover a sufficiently broad range of partial pressures, and extend close enough to the saturation limit.

3.3. Required range of isotherm data

In principle, the isotherm data should be measured over a range of partial pressures that extends to the monolayer saturation. It is important to find out what error can be caused by the truncation of the isotherm data. In Fig. 6, we compare the numerical solution of Eq. 1 with the

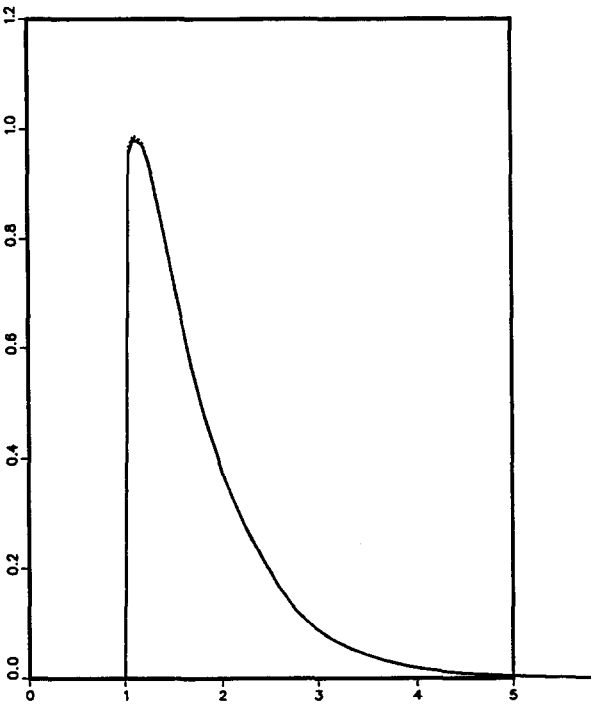

Fig. 4. Comparison of two numerical solutions obtained for the adsorption energy distribution in the case when the experimental isotherm follows a Misra model (Eq. 16). Abscissa, adsorption energy (kcal/mol). Ordinate, energy distribution (mol/kcal). Solid line, adsorption energy distribution calculated with our implementation of the algorithm based on the Adamson and Ling method [25]; dotted line, adsorption energy distribution calculated with our implementation of the HILDA algorithm [26]. The number of iterations in both calculations is 20 000. As expected, there is no difference between the two results.

"experimental" isotherm given by Eq. 16, in three different cases. In the first (solid line), the isotherm data used cover the whole isotherm range. This figure shows that the isotherm data should be acquired from pressures as low as that corresponding to $\epsilon_{max} = 5$ kcal/mol, an up to pressures as high as that corresponding to $\epsilon_{min} = 1$ kcal/mol. In order to investigate the consequences of a truncation of the isotherm data, we carried out two other calculations, using the same isotherm data, but truncated at either low or high pressures.

The energy distribution given by the dotted line was calculated with the same isotherm data, after truncation of the low-pressure isotherm data, the cut point corresponding to $\epsilon = 4$. The

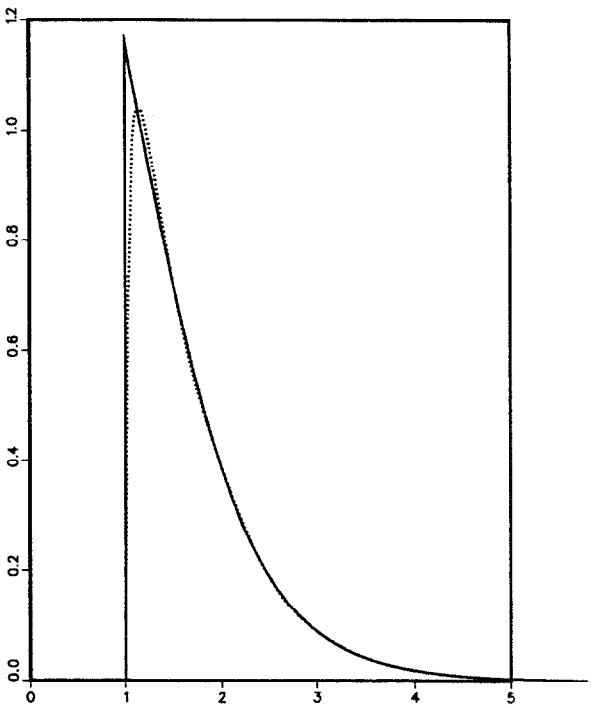

Fig. 5. Comparison of the analytical and numerical solutions obtained for the adsorption energy distribution in the case when the experimental isotherm follows a Misra model (Eq. 16). Abscissa, adsorption energy (kcal/mol). Ordinate, energy distribution (mol/kcal). Solid line, adsorption energy distribution calculated with the analytical solution (Eq. 17); dotted line, adsorption energy distribution calculated with our implementation of the HILDA algorithm [26]. The number of iterations is 20 000.

energy distribution obtained is nearly correct below $\epsilon = 3$, but in serious error above, and even making no sense for energies exceeding 4 kcal/mol. Missing the data corresponding to the high-energy sites has relatively little effect on the energy distribution for the low-energy sites. Conversely, the dashed line shows the energy distribution calculated using the same isotherm data, after truncation of the high-pressure part, corresponding to adsorption energies lower than $\epsilon_{min} = 2$. The energy distribution obtained in this case is made of three sharp peaks, and could be mistaken for a distribution corresponding to a tri-Langmuir isotherm. It has nothing in common with the "true" energy distribution (solid line).

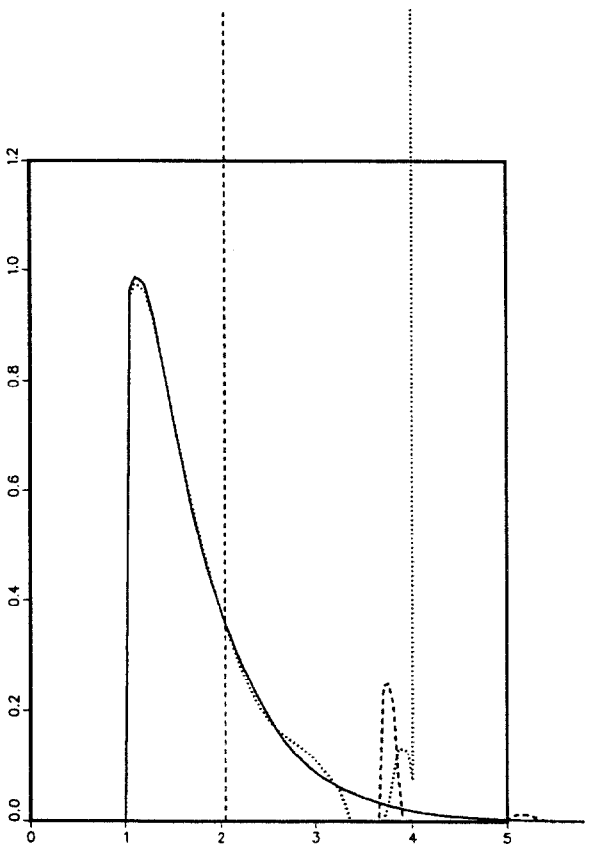

Fig. 6. Effect of the range of isotherm data acquired for the calculation of the adsorption energy distribution. Abscissa, adsorption energy (kcal/mol). Ordinate, energy distribution (mol/kcal). Comparison of numerical solutions obtained for the adsorption energy distribution in the case when the experimental isotherm follows a Misra model (Eq. 16). In this instance, the isotherm data used in the program include the whole range of partial pressures up to the saturation capacity. Dotted line, adsorption energy distribution calculated with isotherm data truncated at low pressures and complete at high pressures, so the data include all those corresponding to an adsorption energy lower than $\epsilon_{max} = 4.0$ kcal/mol; dashed line, adsorption energy distribution calculated with isotherm data truncated at high pressures but complete at low pressures, so the isotherm data include those corresponding to an energy higher than $\epsilon_{min} = 2$ kcal/mol.

These results show how important it is to acquire isotherm data up to very high values of the adsorbate partial pressure. The lack of measurements carried out in a sufficiently wide

partial pressure range results in erroneous adsorption energy distributions, and leads to incorrect conclusions.

4. Conclusions

The Sips method gives the only analytical solution that corresponds to a Langmuir model for the local isotherm, but it requires that we use one of the few isotherm models for which it can be solved to account for the experimental adsorption data and it cannot be applied directly to the experimental adsorption isotherm. For that, a numerical solution is necessary [1,2]. Such a solution does not require any model for the experimental isotherm data, but uses directly the experimental data, and has the further advantage of being able, at least in principle, to accommodate any local isotherm model.

The availability of an analytical solution in a non-trivial case, however, is extremely helpful as a benchmark for the numerical solutions. The implementation of these solutions requires a large number of iterations. Such calculations introduce numerical errors, usually in the form of dispersive contributions. The comparison between the energy distributions resulting from a numerical solution and from the corresponding analytical solution, when it exists, gives a useful performance index of the numerical procedure used. From this point of view, both the Adamson–Ling and the HILDA algorithms are satisfactory.

Finally, the computer simulation of an entire experiment performing the determination of the adsorption energy distribution on a surface with an assumed distribution permits the determination of the specifications regarding the experimental parameters selected and the study of the systematic errors introduced by experimental procedures (*e.g.*, temperature or flow-rate). Both numerical methods studied here require the determination of isotherm data up to irrealistically high values of the partial pressure of the adsorbate.

5. Acknowledgements

This work was supported in part by Grant DE-FG05-88ER13859 of the US Department of Energy and by the cooperative agreement between the University of Tennessee and the Oak Ridge National Laboratory. We acknowledge support of our computational effort by the University of Tennessee Computing Center.

6. References

[1] W. Rudzinski, D.H. Everett, *Adsorption of Gases on Heterogeneous Surfaces*, Academic Press, New York, 1992.
[2] M. Jaroniec and R. Madley, *Physical Adsorption on Heterogeneous Solids*, Elsevier, Amsterdam, 1988, Ch. 2 and 3.
[3] T.L. Hill, *J. Chem. Phys.*, 17 (1949) 762.
[4] S. Ross and J.P. Oliver, *On Physical Adsorption*, Interscience, New York, 1964.
[5] R.R. Zolandz and A.L. Myers, *Prog. Filtr. Sep. Sci.*, 1 (1979) 1.
[6] L.M. Dormant and A.W. Adamson, *Surf. Sci.*, 62 (1977) 337.
[7] W.A. House, *J. Colloid Interface Sci.*, 67 (1978) 166.
[8] P.H. Merz, *J. Comput. Phys.*, 38 (1980) 64.
[9] G.F. Miller, in J. Walsh and L.M. Delves (Editors), *Numerical Solutions of Integral Equations*, Clarendon Press, Oxford, 1974, Ch. 13, p. 175.
[10] R. Sips, *J. Chem. Phys.*, 18 (1958) 1024.
[11] J.P. Hobson, *Can. J. Phys.*, 43 (1965) 1934.
[12] L.B. Harris, *Surf. Sci.*, 10 (1968) 129.
[13] J.H. De Boer, *The Dynamic Character of Adsorption*, Clarendon Press, Oxford, 1953, Ch. IV.
[14] L.M. Dormant and A.W. Adamson, *J. Colloid Interface Sci.*, 38 (1972) 285.
[15] D.W. Widder, *The Laplace Transform*, Princeton University Press, Princeton, NJ, 1946, p. 340.
[16] D. Graham, *J. Phys. Chem.*, 57 (1953) 665.
[17] J. Roles and G. Guiochon, *J. Phys. Chem.*, 95 (1991) 4098.
[18] D.N. Misra, *J. Chem. Phys.*, 52 (1970) 5499.
[19] M.M. Dubinin and L.V. Radushkevich, *Dokl. Akad. Nauk SSSR*, 55 (1947) 331.
[20] D.N. Misra, *J. Surf. Sci.*, 18 (1969) 367.
[21] S.E. Hoory and J.M. Prausnitz, *Surf. Sci.*, 6 (1967) 337.
[22] B. Kindel, R.A. Pachovsky, B.A. Spencer and B.W. Wojciechowski, *J. Chem. Soc., Faraday Trans. 1*, 69 (1973) 1162.
[23] M. Jaroniec, X. Lu and R. Madey, *J. Phys. Chem.*, 94 (1990) 5917.

[24] M.J. Sparnaay, *Surf. Sci.*, 9 (1968) 100
[25] R.H. Van Dongen, *Surf Sci.*, 39 (1973) 341.
[26] A.W. Adamson and I. Ling, *Adv. Chem. Ser.*, 33 (1961) 51.
[27] W.A. House and M.J. Jaycock, *J. Colloid Polym. Sci.*, 256 (1978) 52.
[28] S. Ross and I.D. Morrison, *Surf. Sci.*, 52 (1975) 103.
[29] A.T. Hope, C.A. Leng and C.R.A. Catlow, *Proc. R. Soc. London, Ser. A*, 424 (1989) 57.
[30] R.S. Sacher and I.D. Morrison, *Surf. Sci.*, 70 (1979) 153.
[31] J. Roles, M. Kevin and G. Guiochon, *Anal. Chem.*, 64 (1992) 25.
[32] J. Roles and G. Guiochon, *Anal. Chem.*, 64 (1992) 32.
[33] H. Akima, *J. Am. Ceram. Soc.*, 17 (1970) 589.